11-11-2021

Let It Rip: The Mechanics Of Self-Bisection In Asexual Planarians Determines Their Population Reproductive Strategies

T. Goel

Danielle Ireland
Swarthmore College, dhagstr1@swarthmore.edu

Vir Shetty , '22

See next page for additional authors

Recommended Citation

T. Goel; Danielle Ireland; Vir Shetty , '22; Christina Rabeler; P. H. Diamond; and Eva-Maria S. Collins. (2021). "Let It Rip: The Mechanics Of Self-Bisection In Asexual Planarians Determines Their Population Reproductive Strategies". *Physical Biology*. Volume 19, Issue 1. DOI: 10.1088/1478-3975/ac2f29
https://works.swarthmore.edu/fac-biology/673

PAPER

Let it rip: the mechanics of self-bisection in asexual planarians determines their population reproductive strategies

Let it rip: The mechanics of self-bisection in asexual planarians determines their population reproductive strategies

Tapan Goel[a], Danielle Ireland[b], Vir Shetty[c], Christina Rabeler[b], Patrick H. Diamond[a] and Eva-Maria S. Collins[a,b,c*]

[a]Physics Department, UC San Diego, La Jolla, CA, USA
[b]Biology Department, Swarthmore College, Swarthmore, PA, USA
[c]Physics and Astronomy Department, Swarthmore College, Swarthmore, PA, USA

*Corresponding author: Eva-Maria S. Collins (ecollin3@swarthmore.edu)

Abstract
Asexual freshwater planarians reproduce by transverse bisection (binary fission) into two pieces. This process produces a head and a tail, which fully regenerate within 1-2 weeks. How planarians split into two offspring - using only their musculature and substrate traction – is a challenging biomechanics problem. We found that three different species, *Dugesia japonica, Girardia tigrina* and *Schmidtea mediterranea*, have evolved three different mechanical solutions to self-bisect. Using time lapse imaging of the fission process, we quantitatively characterize the main steps of division in the three species and extract the distinct and shared key features. Across the three species, planarians actively alter their body shape, regulate substrate traction, and use their muscles to generate tensile stresses large enough to overcome the ultimate tensile strength of the tissue. Moreover, we show that *how* each planarian species divides dictates how resources are split among its offspring. This ultimately determines offspring survival and reproductive success. Thus, heterospecific differences in the mechanics of self-bisection of individual worms explain the observed differences in the population reproductive strategies of different planarian species.

Keywords: planarian, fission, reproductive strategies, biomechanics

1. Introduction

Freshwater planarians – famous for their regenerative potential – are free-living, soft bodied invertebrates (1). Their slender body structure (length ~ 3-30 mm, width ~ 1-2 mm and height ~ 0.3-0.5 mm) leads to a large surface area-to-volume ratio, allowing planarians to function without a circulatory system: oxygen is absorbed through the body wall and nutrients are

absorbed via a muscular feeding tube (pharynx) in the mid-region of the body that connects to an extensive digestive tract (1). Like many other soft bodied animals, they maintain their body shape via a dense network of circular, longitudinal and diagonal muscle fibers and hydrostatic pressure from internal fluids (2).

Some species of freshwater planarians reproduce asexually by ripping themselves transversally into a head and a tail piece, which then regenerate the missing body parts. How planarians self-bisect – using only their musculature and substrate traction – is an intriguing biomechanics problem that even sparked the interest of Michael Faraday (3). However, study of this behavior has been hindered by its experimental inaccessibility. There are no known inducers of planarian division and the time between divisions (reproductive waiting time (RWT)) can range from a few days to many months (table S1), making it impossible to predict when a planarian will divide. Moreover, planarians will abort the division process upon any type of disturbance. Therefore, many studies have focused on the population level to gain insights into planarian reproductive dynamics (4–9).

Long-term population studies have revealed that *how* planarians split up their body and allocate biomass among their offspring determines the offspring's survival and reproductive success. Previous work has shown that *Dugesia japonica* (J-planarians), *Schmidtea mediterranea* (S-planarians) and *Girardia tigrina* (G-planarians) allocate resources differently among their offspring (table S1, area at birth). Interestingly, area at birth – not area at division – determines offspring survival outcomes and population growth dynamics (7,8). J-planarians reproduce ("fission") approximately once every month. Both offspring types have narrow distributions of RWTs, with the larger head offspring dividing on average twice as fast as tail offspring. Both offspring have negligible death rates (7). In contrast, S-planarians display wide RWT distributions for both head and tail offspring, with tail offspring dividing on average only once every 2.5 months. S-planarian offspring death rates are significantly higher than J-planarian offspring death rates (7). The dramatic head/tail differences in RWTs and mortality rates are a consequence of the reproductive strategy of S-planarians. The majority of S-planarians "fragment": individuals produce one or more trunk (middle piece) offspring within 5 days after the first division – i.e., before regeneration is complete (figure S1). These middle pieces are comparable to tail offspring in size and reproductive behavior (4). Finally, G-planarians display a third strategy: They allocate their resources primarily to the head offspring (7). This allows the head offspring to divide the most rapidly of all 3 species (on the order of once every 2 weeks). This rapid reproduction comes at the cost of small tail offspring with the highest death rates (table S1). Notably, the population reproductive strategies of J- and G-planarians have previously been described using mixed models of timer, adder, and sizer strategies (8). Moreover, while population growth rates are affected by feeding frequency (5), population density and competition between species (7), these parameters do not change the underlying mode of division or the relative biomass allocation among offspring.

Two recent studies on the mechanism of self-bisection of J-planarians (10) and S-planarians (11) have used large-scale, long-term imaging to record self-bisection. They found that these two species split using different biomechanical mechanisms. J-planarians use rhythmic pulsations of the anterior end to create longitudinal stress in the waist. Using traction force measurements, Malinowski et al. showed that two opposing traction forces act to generate a tensile stress in the waist, on the order of 2000 Pa immediately before rupture (10). The rupture location for J-planarians was found to be determined by the position of the pharynx and by substrate friction (10). Arnold et al. showed that S-planarians elongate to create tension in the waist and proposed that in S-planarians the division plane is pre-specified through the existence of mechanical weak spots that can be identified via mechanical compression. These "compression planes" are distributed equidistantly along the head-tail axis (11). Their number and spacing is influenced by Hox gene expression patterns (12). The spacing between compression planes was found to be independent of S-planarian length, but the number of compression planes was positively correlated with length. This theory can explain the observations that S-planarian tail offspring length appears to be independent of parent length (11) and that larger S-planarians tend to make more offspring (4). However, this is impossible to test directly as observation of compression planes requires killing the planarian.

Given that J- and S-planarians have similar tissue mechanics and are both limited by the same constraints of using only their musculature and substrate adhesion to divide, we found it surprising that they have evolved such different solutions to tear themselves apart. Because S-, J- and G-planarian species differ in their reproductive strategies (7), we hypothesized that each species had evolved a distinct mechanism of self-bisection tailored to their unique reproductive strategies. To test this, we first characterized and quantified how individual planarians of the three species self-bisect at unprecedented spatial and temporal resolution. This provided the first quantitative description of the kinematics of G-planarians self-bisection and the necessary quantitative parameters of S-planarian self-bisection, which were lacking in previous studies. We observed key differences in how the tensile stress required for division is generated in each species. However, we also identified two conserved features that are indispensable for planarian self-bisection: (1) the formation of a local constriction, or "waist", to amplify the tensile stress and (2) the formation of adhesion patches anterior and posterior to the waist to prevent slipping and to maintain stress in the waist. Using a simple biomechanical argument and experimental data, we can predict where the waist forms in J- and G-planarians and demonstrate how anatomical constraints can explain why these species rarely fragment. Our results link the minute-long individual-level mechanics of planarian division to the generational, weeks-long reproductive behavior of the population. We show that *how* individual planarians self-bisect can explain much of the reproductive strategies of the different planarian species.

2. Materials and methods

2.1. Planarian maintenance

Clonal asexual *Dugesia japonica* (J-planarians)*, Schmidtea mediterranea* (S-planarians)*,* or *Girardia tigrina* (G-planarians) were used for all experiments. Planarians were stored in Tupperware containers in the dark in a temperature-controlled Panasonic incubator at 20°C. J- and G-planarians were kept in 0.5 g/L Instant Ocean Salts (Spectrum Brands, Blacksburg, VA, USA). S-planarians were kept in 1x Montjuic salts (13). The solution used for each respective species will be referred to as "planarian water" and can be considered equivalent media. It has previously been shown that using slightly different planarian water formulations does not change the fission dynamics of J-planarians (10). Planarians from all species were fed organic beef liver from a local farm 1-2 times per week. Worms were cleaned 2 h and again 2 days after feeding and starved for at least 5 days before being used for experiments.

2.2 Experimental considerations

Planarian self-bisection is difficult to study due to the different time scales involved in the process. The timescale of interest for investigating the mechanics of self-bisection (as shown in this study) ranges from ~0.1 second (to study tissue rupture) to tens of minutes (to study elongation and waist formation). However, as shown in table S1, reproduction naturally occurs on average only about 1 in 20 days, with some worms not dividing for months, making it impossible to predict when a given planarian will divide. The long timescales prevent us from physically constraining planarians and waiting for division, as worms would get sick under such conditions and no longer divide. Thus, we monitored and recorded hundreds of planarians that were freely moving around in a few cm wide arenas (see section 2.3) for several months to obtain the reproductive events that were quantified here. This setup meant that we could not simultaneously image dividing planarians from the top and the side to get volumetric measurements. From separate side and top view recordings, we made assumptions and simplifications of the planarian body shapes. Because these assumptions were made for all 3 species, these do not change the relative differences. Furthermore, we continuously recorded at high frame rates and resolution, generating terabytes of data, because attempts to use body shape changes to detect the onset of division were not fruitful. There are no known inducers of planarian self-bisection. However, planarians were decapitated, because decapitation has been reported to increase the likelihood of division in the presence of light (14) and a brain is not necessary for self-bisection. Cuts were performed with a clean razor blade perpendicular to the head–tail axis and as close to the head as possible. No differences were observed in the division dynamics between intact and decapitated animals (Movies S1- S3). Therefore, we will use the term 'head" to denote the anterior end for both decapitated and intact specimen. Because planarians cease to divide upon the slightest disturbance, they cannot be manipulated directly. If disturbed, self-bisection comes to an abrupt halt, and depending on where in the process the disturbance occurs, can result in a plastic deformation of the body at the site where division would have occurred (figure S2(a)). Contrary to older claims of contact inhibition preventing

division (15–18), we found that in all three species physical contact with conspecifics did not prevent division (figure S2(b-d)). So, recording was done at low density conditions so that overlapping planarians did not obstruct tracking of individuals' division dynamics.

2.3. Video recording of reproduction

Videos of reproduction events were recorded similar to (10) using either a Flea3 USB3 or a Grasshopper USB3 camera (FLIR Systems Inc., Wilsonville, OR), mounted on ring stands and controlled by a custom MATLAB 2019a (MathWorks, Natick, MA, USA) script. Images were recorded at 7-10 frames per second (fps). Three to four experimental setups were run in parallel, each containing 2-4 planarians, depending on the size of the arena (wells of 6-well plates, 30 mm petri dishes, contact lens containers (19), or Polydimethylsiloxane (PDMS) blocks (10). For high-resolution imaging of rupture, we used 2 planarians in contact lens containers (Wohlk Contactlinsen GmbH, Schonkirchen, Germany). Planarians were replaced after division or at least every week. The wells were replenished with planarian water twice every day to account for evaporation loss. Total water exchanges happened at least 1x/week.

Lengths and areas of various regions in dividing planarians were quantified from the video recordings using built-in tools (thresholding, analyze particles, skeletonize) in the Fiji distribution of ImageJ (20). The widths of various parts of the worm – adhesion patches, waist, resting width – were measured manually using the line tool (figure S3(a)). Because the waist region is thinner than neighboring regions, it is easily identified via its shape and its higher pixel brightness values. In contrast, adhesion patches were identified as darker tissue regions (lower pixel values due to increased tissue density (10)) immediately anterior and posterior to the waist that did not start moving immediately before or after waist rupture was complete.

Custom MATLAB scripts were used to measure the body lengths and areas of the planarians during division as functions of time. The scripts and corresponding documentation are available at https://github.com/Collinslab-swat/LetItRip. Briefly, the images of the worms were first binarized by thresholding grayscale values. The centerline and center of mass of the binarized image were identified using standard MATLAB functions. The head and tail along the centerline were defined manually for the first image and then tracked using a nearest neighbor algorithm in successive images. The shape of the worm was parameterized as the distance between points on the centerline to their respective nearest points on the boundary of the worm. These steps were applied to each image, using nearest neighbor tracking to track a single individual.

2.4. Imaging S-planarian offspring post-reproduction

Planarians were maintained individually in 100 mm plastic petri dishes (Simport Scientific) in approximately 25 ml planarian water and fed and cleaned as described in section 2.1. Planarians were imaged individually 0-3 days post-division in their respective dishes using a Leica stereo

microscope (Leica Microsystems, Wetzlar, Germany) equipped with a Flea3 USB3 camera (FLIR Systems Inc.) and Pointgrey software.

2.5. Stickiness assay

On Day 0, planarians (approx. 0.5-2 cm length) of each species were loaded into 48-well plates (Genesee Scientific, San Diego, CA) such that each well contained one planarian and 200 µl of planarian water. Relative differences in substrate adhesion ("stickiness") were tested by shaking the plate using a fixed rotation speed (452 rotations per minute (rpm) for 3 seconds) on an orbital shaker (Big Bear Automation, Santa Clara, CA) similar to in (21). The plate was imaged from above by a Flea3 USB3 camera mounted on a ring stand and imaged at 20 fps. Each individual planarian was manually scored as either "unstuck" (displaced by the water flow) or "stuck" (not displaced). Planarians which were dead, on the side of the well, or not visible were not scored and excluded from the analysis. After stickiness was assayed on Day 0, the plates were either stored (control) or agitated on an orbital shaker (see section 2.6) for 3 days. Stickiness was assayed again on Day 3. Each species and condition were tested in 3 separate plates with n=24-48 per plate. These data were analyzed in two ways: 1) to compare stickiness between the three species and 2) to compare, within each species, how stickiness changed due to the incubation on the orbital shaker. To compare the stickiness across the three species, we calculated the percentage of control planarians of each species that remained stuck to the substrate after shaking. Thus, populations with a larger percentage of adhered worms were considered "stickier". These population-level comparisons were done with the control populations on Day 3 as G-planarians had much fewer adhered worms when first placed into the multi-well plates (figure S4), possibly due to disruption to the mucus during pipetting.

To compare how stickiness changed due to incubation on the orbital shaker within each species, we scored individual planarians as stuck or unstuck on Day 0 (D0) and Day 3 (D3). We were able to track individual planarians since they were loaded into the 48-well plates with only one worm per well. Thus, to express the change in stickiness over time, each worm was classified as either having increased stickiness (D3>D0, i.e., unstuck on D0 and stuck on D3), decreased stickiness (D3<D0, i.e., stuck on D0 and unstuck on D3) or having the same stickiness on both days (D3=D0, i.e., stuck/stuck or unstuck/unstuck). Statistical significance between groups was determined using a Fisher's exact test comparing the number of planarians with increased stickiness vs the number of planarians with decreased or unchanged stickiness on Day 3 compared to Day 0.

2.6. Centrifugal force experiments

Individual intact planarians were placed in single wells of a tissue culture treated 6-well plate (Genesee Scientific), with each well containing approx. 3 ml planarian water and one planarian. For each experiment, planarians of comparable size (approx. 1-1.5 cm length) were used. Centrifugal forces were introduced using a Spindrive orbital shaker platform (SP Bel-Art,

Wayne, NJ, USA) on a magnetic stirrer. The angular speed of the shaker in rpm was determined using a video recording of the motion with a cell phone camera. Shaking was performed in the dark. The plates were checked every 2-3 days for divisions and divided planarians were exchanged with intact ones. Planarian water was exchanged at least once a week. Planarians were continuously kept on the shaker for a maximum of 3 weeks. Offspring, defined as all the pieces in the dish including the anterior most segment, were imaged in a 100 mm petri dish using a Vividia Andonstar HM-302 digital microscope (Oasis Scientific Inc, Taylors, SC, USA). The offspring were allowed to stretch out and glide before imaging. The areas and lengths of the individual offspring were quantified in Fiji (20). The images were cropped to isolate the worm offspring of interest, converted to greyscale and thresholded to identify the worm from the background. Areas were then measured using the *analyze particles* tool and lengths were measured using the *segmented line* tool. If thresholding was not possible, the *polygon* tool was used. The parent area was calculated as the sum of the offspring areas. For each speed setting (J-planarians: 0, 70 and 100 rpm, G-planarians: 0, 100, 120 and 140 rpm, and S-planarians: 0, 100 and 120 rpm), a new set of planarians was used.

2.7. Predicting number of offspring

J-planarian offspring were imaged using a Leica stereo microscope (Leica Microsystems) with a Basler A601f CCD camera (Basler AG, Ahrensburg, Germany) and Basler Pylon Viewer. G-planarian offspring resulting from a fission were imaged as in section 2.6. The location of the pharynx was determined manually, and the area of the offspring was divided into pre-pharyngeal, pharyngeal, and post-pharyngeal areas (figure S3(b)).

To predict whether a G-planarian would fragment or not, the post-pharyngeal area of the head offspring was measured. If this area was greater than 25% of the area of the head offspring, we assumed that this head offspring could fragment.

For J-planarians, we assumed that the worms could fragment if the area of the head offspring was above an absolute minimum area. This minimum cutoff area was estimated from head offspring areas of fragmentation events. From imaging data of trunk and tail offspring of J-planarians, we found that the trunk offspring area scales with the tail offspring area. Based on this scaling relationship, we estimated the size of a theoretical trunk offspring for J-planarians which underwent fission. This theoretical trunk area was subtracted from the area of the fission head offspring to estimate the size of the theoretical final head offspring resulting from a second division. This theoretical head offspring area must exceed the cutoff head offspring area to permit fragmentation (figure S5).

S-planarian offspring from fissions and fragmentations were imaged as in section 2.4. To predict the number of offspring an S-planarian could produce, we divided the parent worm area by the average area of the tail offspring and compared it to the actual observed number of offspring of the same S-planarians.

2.8. Data analysis

Data from video recordings and centrifugal force experiments were analyzed using MATLAB 2021a (MathWorks, Natick, MA, USA). Linear regressions were conducted using the fitlm function in MATLAB. Statistical tests were conducted using inbuilt MATLAB functions. Parameters obtained from linear fits and normally distributed data are reported as mean ± standard deviation and compared using the 2-sample t-test (ttest2 in MATLAB). All other parameters and non-normal data are reported as median (25^{th} percentile, 75^{th} percentile) and compared using the Wilcoxon rank sum test which is equivalent to the Mann Whitney U-test (ranksum in MATLAB). Root mean squared errors were calculated as described in supplementary methods. For measurements of lengths and areas during fission in *D. japonica*, data published in (10) were also used in addition to new measurements made as described in the preceding sections. Population data such as RWTs of head and tail offspring, and their areas at birth, previously published in (7) was also used in addition to our newly acquired data.

3. Results

3.1. The kinematics of planarian division

Using video recording at unprecedented spatial and temporal resolution, we observed the details of how individual planarians of the three species (J-, G-, and S-planarians) self-bisect. Across species, the tensile stress needed for rupture is created through elongation and amplified using local constriction. Asexual reproduction can be divided into 4 phases (figure 1): Rest (Phase 0); Initiation (Phase 1); Stress Localization, with a distinct hourglass shape (waist formation; Phase 2); and Rupture (Phase 3). We will briefly summarize how each species divides and then compare the different mechanisms for each phase.

3.1.1. J-planarians

As previously shown (10), J-planarians begin to form a waist-like constriction in Phase 1 (figure 1(bi)), mediated by contraction of circular muscles. Waist formation is completed during Phase 2 and is accompanied by the appearance of wide adhesion patches – regions of tissue contact with the substrate – anterior and posterior to the waist. Longitudinal pulsations of the head then build tensile stress in the waist (10). The head experiences large length changes of about 40% during the pulsations (10), which generates the longitudinal stress in the waist that is necessary for rupture (10). In Phase 3, the waist ruptures once the longitudinal stress exceeds the ultimate tensile strength of the tissue, and division is complete.

3.1.2. G-planarians

While division in G-planarians shares key steps with J-planarian division, it displays unique features (figure 1(a)): To initiate division (Phase 1), G-planarians constrict their posterior to form a thin tail, giving them a popsicle-like appearance (figure 1(bii)). Similar to J-planarians, this constriction is achieved through active contraction of circular muscles, because G-planarians maintain this shape while gliding. During Phase 2, a short section of the thinned posterior

adheres to the substrate while the wider anterior continues to move forward, forming a waist region. Head pulsations are not observed. Instead, once a part of the anterior also adheres to the substrate, the tissue in the waist ruptures rapidly.

3.1.3. S-planarians

As described in (11,12), S-planarian division relies on extreme longitudinal extension (figure 1(biii)). While the other two species initiate division by local constriction, S-planarians initiate division by extending their anterior forward while keeping the tail in place. Elongation is followed by waist formation in Phase 2. The head continues to extend while the adhesion patches remain stationary. This extension builds tensile stress, which is amplified by the constriction of the waist, eventually leading to rupture in Phase 3. The kinematics of S-planarian division are the same for divisions producing tail and trunk offspring, suggesting that, for all practical purposes, trunks and tails can be treated the same.

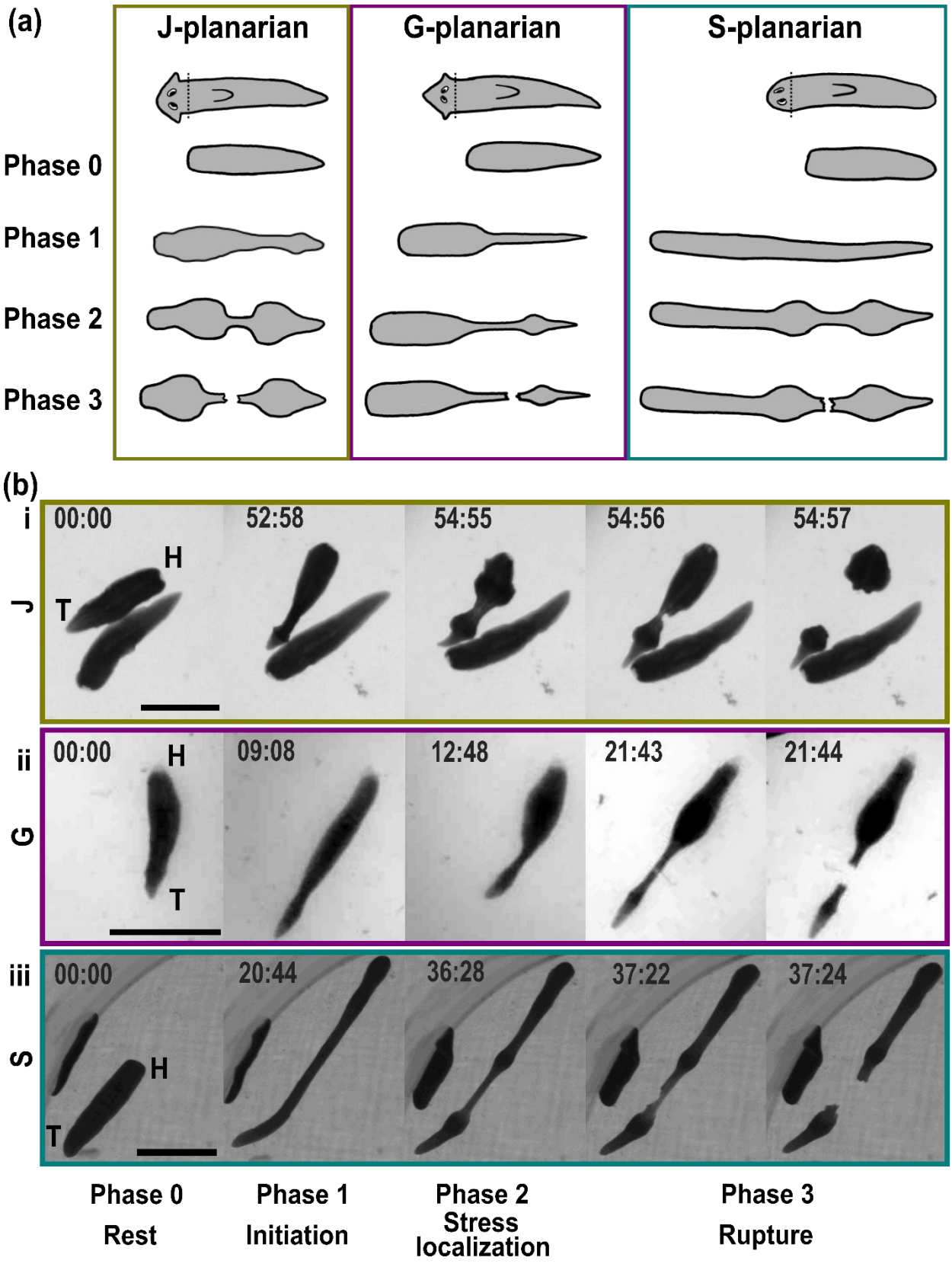
(a)
J-planarian
G-planarian
S-planarian
Phase 0
Phase 1
Phase 2
Phase 3
(b)
i
J
00:00
52:58
54:55
54:56
54:57
H
T
ii
G
00:00
09:08
12:48
21:43
21:44
H
T
iii
S
00:00
20:44
36:28
37:22
37:24
H
T
Phase 0
Rest
Phase 1
Initiation
Phase 2
Stress localization
Phase 3
Rupture

Figure 1. Overview of the division process in J-, G- and S-planarians. (a) Schematic comparing the main phases of division in the 3 species. We decapitated the planarians to increase the likelihood of division in the presence of light. Anterior is to the right. (b) Example image sequences of the phases of division in (i) J-planarians, (ii) G- planarians and (iii) S-planarians. Scale bar: 5 mm. H: head, T: tail. Time stamps are minutes: seconds.

3.2. Phase 1: Initiation

J- and G-planarians initiate division by forming a local constriction (figure 2(a-b)). In J-planarians, the constricted region begins to resemble the distinctive hourglass shape of the future waist (figure 2(a)). In contrast, G-planarians initially constrict almost the entire posterior, assuming a popsicle-like shape (figure 2(b)). J-planarians form the constriction at 69% ± 7% (mean ± standard deviation) and G-planarians at 66% ± 9% of their body length along the anterior-posterior (A-P) axis (figure 2(a-b)). The constricted region will become the waist in Phase 2. Thus, where J- and G-planarians divide and how they allocate resources between offspring is constrained and specified at the onset of fission. In contrast, S-planarians do not constrict during Initiation (figure 2(c)). Instead, S-planarians elongate to almost twice their rest length (figures S6 and 7). This is achieved through a "crawling" motion consisting of successive series of adhesion and de-adhesion (figure S7(a)). This is often accompanied by the formation of undulations where portions of the tissue rise off the substrate (figure S7(a)), previously called "contortions" (12). A-P directed peristaltic waves have been observed concomitantly with the formation of these undulations (12). Peristalsis (22) is induced by compression of planarian longitudinal muscles. Therefore, we suspect that these undulations are a result of the planarian body buckling under compressive forces generated by the longitudinal muscles. The S-planarian elongation process follows a characteristic sigmoidal time course (Supplementary text 1, figure S6). J- and G-planarians do not elongate (figure S7(b, c)).

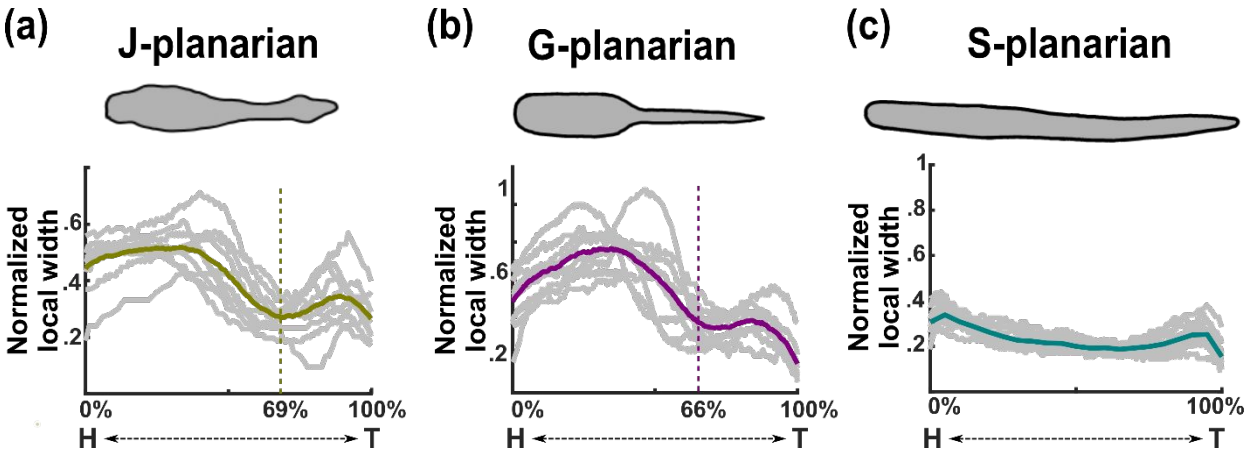

Figure 2. Phase 1 – Initiation. (a-b) Local width, normalized to the rest width, along the normalized length of the planarian for a) J-planarians (n=10), b) G-planarians (n=9) and c) S-planarians (n=13). Data

for individual planarians are shown as grey lines. The average is shown as a green, magenta, and blue line for (a), (b) and (c), respectively. Dotted lines denote the local minimum normalized width, averaged over all gray curves. Note that S-planarians do not create a local minimum.

3.3. Phase 2: Stress Localization

Waist formation is critical to self-bisection. It localizes and amplifies tensile stress through the large difference in cross-sectional area between the narrow waist and the wide adhesion patches. The adhesion patches pull on either side of the waist, generating tensile stress in the waist. In turn, the adhesion patches feel a tensile force due to the waist, balanced by the friction between the substrate and the adhesion patches, which sets the upper limit to the tension force that the adhesion patches can exert on the waist. While the magnitude of the tension force is the same for the (posterior) adhesion patch and the waist, the smaller cross-sectional area of the waist means that it experiences a larger stress. This increased stress due to the same tension force is quantified by a multiplicative stress amplification factor, calculated from the ratio of the cross-sectional areas of the adhesion patch and the waist (Supplementary methods). Estimates of the stress amplification factor (figure 3 and figure S8(a-c)) were similar for S- and G-planarians ($p > 0.05$, unpaired 2-tailed t-test) but significantly higher in J-planarians ($p < 0.01$, unpaired 2-tailed t-test). However, the ultimate tensile strength of the waist - estimated from the product of the stress amplification factor and the linear strain (Supplementary methods) – is not statistically different across the three species (J-planarians: 3.2 ± 2.7, G-planarians: 3.2 ± 1.7 and S-planarians: 5.3 ± 2.0 (mean ± root mean squared error), $p > 0.05$, 2-tailed t-test). It is expected that the species have similar tensile strengths, given their similar tissue properties.

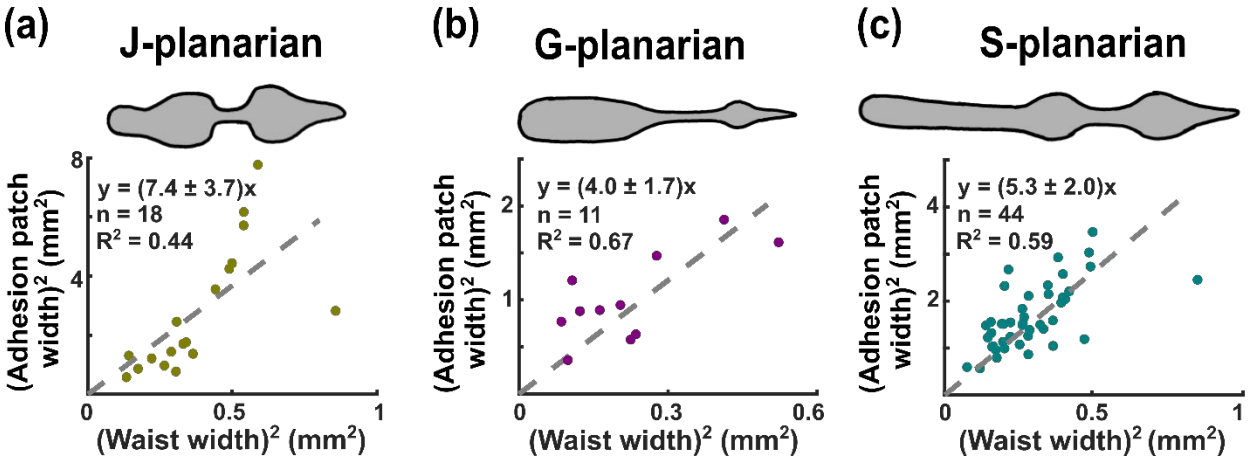

Figure 3. Phase 2 – Stress localization. (a-c) The square of the tail adhesion patch width plotted against the square of the width of the waist for a) J-planarians, b) G-planarians and c) S-planarians. Dashed lines represent linear fits. The slopes (shown as mean ± std) are used as estimates of the stress amplification factor.

For J- and G-planarians, waist formation is driven by active contraction of muscles. The initial constriction that appears during Phase 1 takes on the distinctive hourglass shape in Phase 2 when the adhesion patches form. Substrate adhesion is not necessary to create or maintain the waist in J- and G-planarians. This idea is supported by the observation that in both species, the shape of the waist is maintained even as the planarian continues to glide on the substrate and even after one of the adhesion patches slips and the tension is decreased (figure S9(a, b)). However, substrate adhesion is indispensable for S-planarian waist formation. If one of the adhesion patches slips, the waist disappears, the S-planarian fails to rupture and must start elongating all over again (figure S2; figure S9(c)). Additionally, S-planarians frequently form several adhesion patches, resulting in formation of multiple evenly spaced temporary waists (figure S9(d)). Eventually, one of these waists remains and the others disappear. This behavior suggests that in S-planarians: 1) waist formation is a passive result of elongation and, 2) there appear to be multiple possible division planes which are evenly spaced, consistent with the presence of compression planes (11).

All three species use active, longitudinal motion to stretch the waist and build the necessary stress to initiate rupture. However, the three species use distinct mechanisms: J-planarians use asymmetric longitudinal head pulsations (10), G-planarians stretch their waist by attaching the tail to the substrate while the head moves away, and S-planarians continue to elongate, which stretches and thins the tissue in the waist (figure 1(biii)). Importantly, substrate adhesion is critical for all these processes to build the tensile stress in the waist necessary for rupture. Substrate adhesion and behaviorally mediated tensile stress generation are also important for transverse fission in some species of acoels (23), suggesting that these are key, conserved aspects of self-bisection.

3.4. Phase 3: Rupture

Once the stress in the waist exceeds the ultimate tensile strength of the tissue, the tissue ruptures (figure 4(a)). A small defect forms somewhere within the waist and then propagates across the waist until rupture and division are complete. The rupture process is significantly slower in S-planarians (2.9 (1.4,8.0) s, median (25^{th}, 75^{th} percentiles), $n = 44$, $p < 10^{-4}$, Wilcoxon rank sum test) than in J- and G-planarians (0.5 (0.2,1.0) s, $n = 14$; 0.4 (0.2,0.7) s, $n=12$, respectively) (figure 4(a)). To characterize the force balance within the waist, we compared the location of the initial rupture site in each species. Along the medio-lateral axis, all three planarian species showed rupture initiation at both the center and at the lateral edge of the waist (figure 4(b)). This suggests that fracture nucleation is not tied to a fixed anatomical feature. For all species, the rupture plane lies close to the center of the waist along the A-P axis irrespective of the length of the waist (figure S10). This suggests that the tensile forces on either end of the waist must be equal and opposite, assuming the tissue in the waist itself is homogeneous.

After rupture, the stretched tissue on either side of the rupture plane passively recoils to release the stored elastic energy. For all three species, the separation between the recoiling tissues follows an exponential saturation in time (figure 4(c)). This recoil could be active or passive movement. While we cannot rule out contribution from active motion because we cannot visualize muscle activity during self-bisection, the exponential saturation suggests that the recoil is passive viscoelastic relaxation. Thus, treating the tissue as a Kelvin-Voigt material, we obtain relaxation times from the exponential fits, which are similar for J- and G-planarians ($p > 0.05$, Wilcoxon rank sum test) but significantly larger for S-planarians ($p < 0.001$, Wilcoxon rank sum test) (figure 4(c)).

The longer timescales observed in S-planarians, both for rupture and for recoil, suggest that the drag forces for S-planarians are larger than the other two species. Notably, the waist region is not in contact with the substrate during rupture and recoil (figure S7(a)) and only interacts with the water surrounding it, which can be neglected. Therefore, since relaxation time = viscosity/Young's modulus, the longer timescales suggest increased viscosity of the S-planarian waist tissue or a decreased Young's modulus of the S-planarian tissue compared to the other species, either due to actual differences in material properties or, more likely, due to changes in properties induced during the division process. Imaging at a higher spatial and temporal resolution is needed to uncover the microscopic details of the fracture process – both to study fracture initiation and fracture propagation.

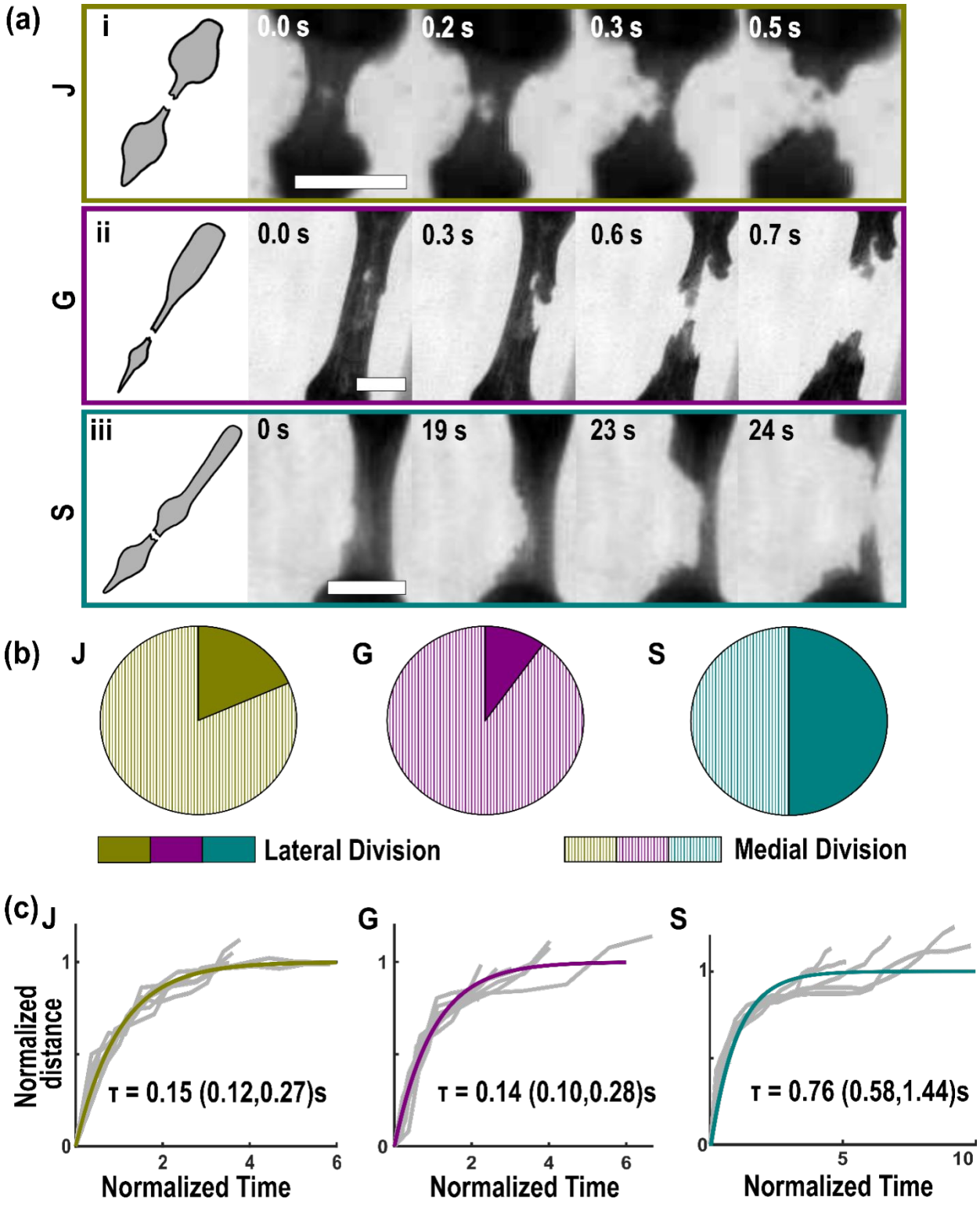

Figure 4. Rupture dynamics. (a) Example image sequence of rupture for a (i) J-planarian, (ii) G-planarian and (iii) S-planarian. Scale bar: 1 mm. (b) Fraction of medial and lateral rupture initiations for J-planarians (n = 25), G-planarians (n = 10) and S-planarians (n = 36). (c) Normalized distance between recoiling tissue pieces post-rupture as a function of normalized time for J-planarians (n = 12), G-

planarians (n = 12) and S-planarians (n = 12). The grey lines indicate normalized recoil curves for each planarian. The colored solid lines indicate the curve $y = 1 - e^{-t}$. τ is the viscoelastic relaxation timescale reported as median (25th percentile, 75th percentile).

3.5. Biomechanical constraints govern offspring size and number

3.5.1. Offspring area scales with parent area in J- and G-planarians but not S-planarians

In J- and G- planarians, which primarily reproduce through fission, the area of the tail offspring scales linearly with parent area (figure 5(a-b)). The slopes in figure 5 correspond to the fraction of parent area that forms the tail offspring. In contrast, in S-planarians, which primarily reproduce through fragmentation creating multiple offspring, tail offspring area is largely independent of the parent area and instead roughly constant (figure 5(c)). Similar results were also found for trunk offspring of S-planarians and when using length as a measure of size instead of area (figure S11), consistent with previous reports (4,6,11).

Notably, these relationships suggest that given the area of the parent, one can predict the size of the tail offspring for all three planarian species.

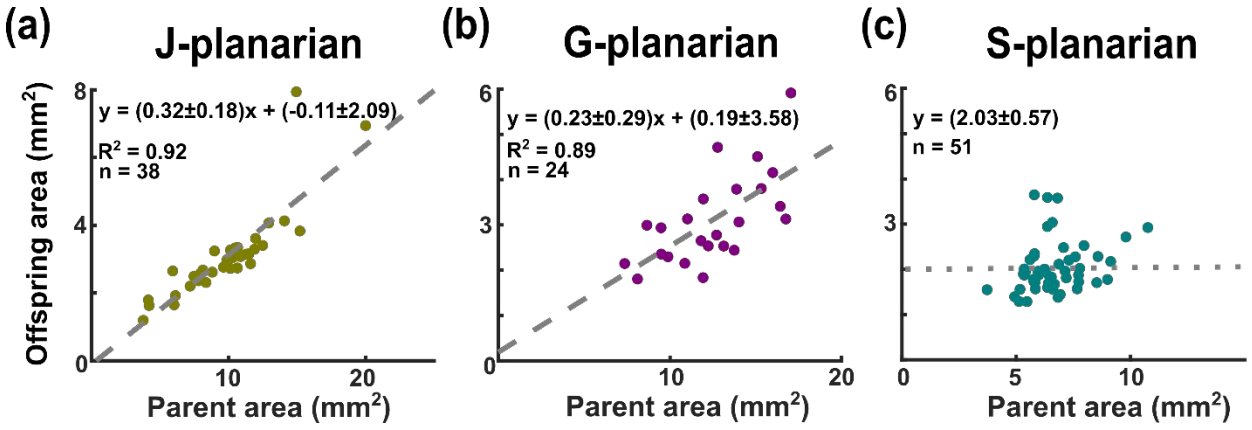

Figure 5. Planarian tail offspring area as a function of parent area. Tail offspring area plotted against parent area for (a) J-planarians, (b) G-planarians and (c) S-planarians. Linear fits are shown as dashed grey lines in (a) and (b). Slope and intercept for the fits are provided as mean ± standard deviation. Dotted line in C indicates average offspring area for S-planarians (mean ± standard deviation).

3.5.2. Planarians modulate substrate adhesion to maintain offspring size

Regenerating J-, G- and S-planarians show differences in relative substrate adhesion or "stickiness", with G-planarians being the stickiest and J-planarians the least sticky (21). This trend is also true for intact planarians (figure 6(a)). This trend in relative stickiness (J<S<G) is

anti-correlated with relative tail offspring size (G<S< J) (7), i.e., the smallest tail offspring is created by the planarian species with the greatest stickiness (G-planarians). This observation suggests that with greater stickiness, a smaller adhesion patch area (and therefore a smaller tail offspring) is required for division. We tested how changing the effective tensile force, achieved by culturing planarians on an orbital shaker rotating at fixed angular frequencies, affected tail offspring area, relative to the static condition.

Increasing angular frequencies would introduce larger centrifugal forces on the planarians. Considering the forces acting on the region posterior to the waist, which is at rest relative to the substrate at the time of rupture, the centrifugal force, the friction due to substrate adhesion and the tension from the waist need to balance out. To prevent slipping, the planarians would have to increase their total substrate adhesion to balance the centrifugal force now acting in addition to the tensile stress on the adhesion patches. We hypothesized that this would require the planarians to make larger adhesion patches and therefore larger tail offspring. However, none of the angular frequencies tested had a biologically meaningful effect on tail offspring area (figure 6(b)). J- and S-planarians placed on frequencies higher than those shown in figure 6 (120 and 140 rpm, respectively) did not divide during the observation time (3 weeks). Additionally, we found that more planarians had increased relative stickiness after being incubated on the shaker at 100 rpm for 3 days than when incubated without shaking (figure 6(c), section 2.5), though this effect was not statistically significant for S-planarians. These results suggest that planarians can actively modulate their stickiness in response to external forces, thus preserving offspring size.

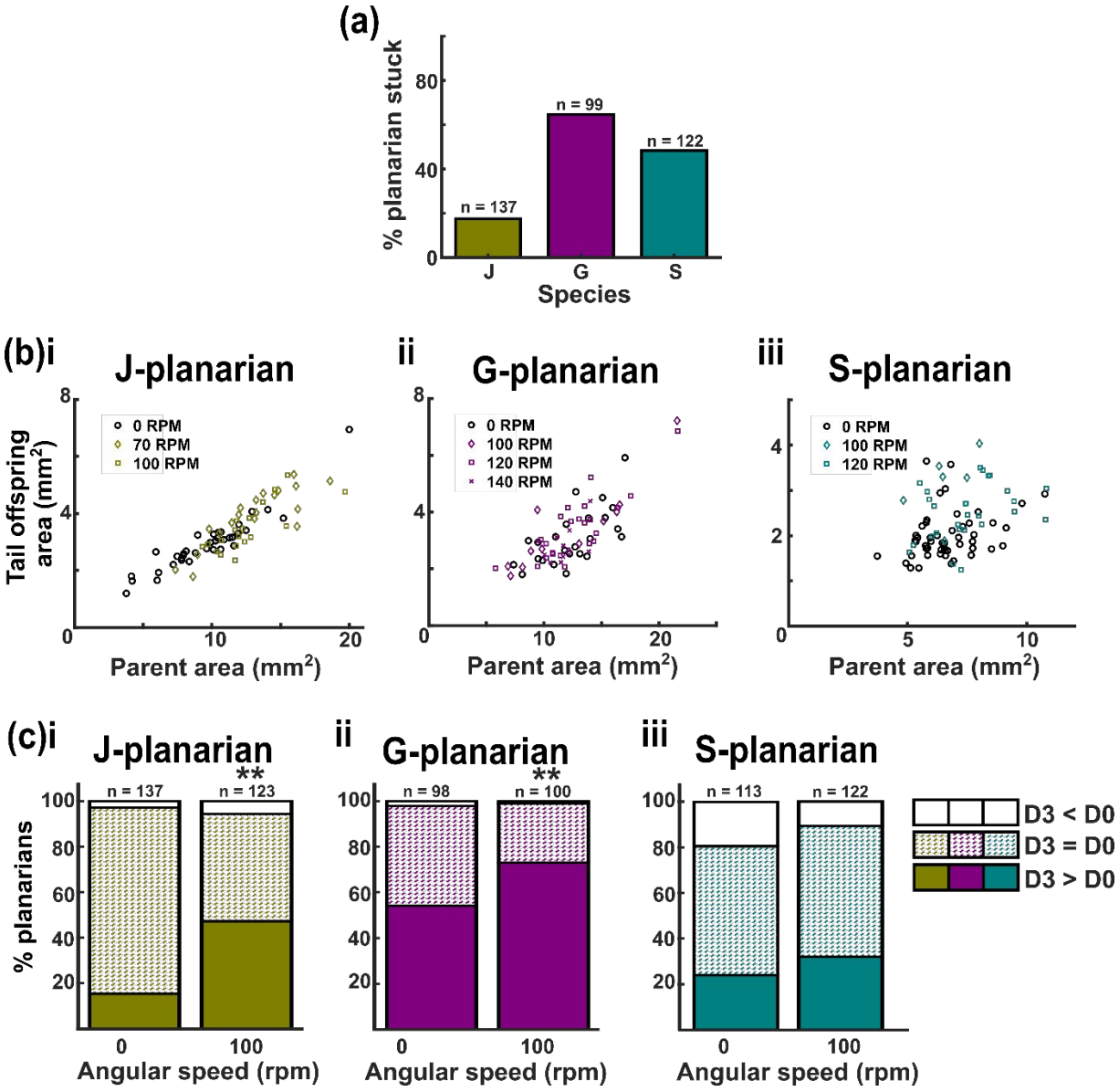

Figure 6. Response to centrifugal forces. (a) Percentage of planarians that remain stuck to the substrate at the end of the stickiness assay. Species with stronger substrate adhesion ("stickiness") have a higher percentage of stuck planarians. (b) Tail offspring area plotted against parent area for planarians that divided while being cultured on an orbital shaker at the specified angular speeds (rpms). No differences in the relationship between tail offspring area and parent area were observed for different angular speeds for any of the three species. (c) Comparison of change in relative stickiness between day 0 (D0) and after 3 days of culturing (D3) at 0 and 100 rpm of (i) J-planarians, (ii) G-planarians and (iii) S-planarians. This data is based on tracking individual worms. Solid bars indicate worms that had increased stickiness on D3, dotted bars indicate worms with the same level of stickiness on D3, and white bars indicate worms with decreased stickiness on D3 (see Section 2.5). (*) denotes $p < 0.05$ and (**) denotes $p < 0.01$ in comparison to the corresponding control (Fisher's exact test).

3.5.3. *Constraints on waist formation mediate offspring number*

Given the differences in the mechanisms of self-bisection between the three planarian species, we sought to determine whether these differences could explain the species' different reproductive strategies (see Introduction, figure S1 and (7)).

3.5.3.1. J-planarians

We observed three biomechanical constraints for J-planarian division. First, the position of the pharynx, a muscular feeding tube in the middle of the planarian body, is a restricted zone in which waist formation and division are not observed (10). About 90% of J-planarian fissions occur post-pharyngeally (figure 2(a) and (10)). If the post-pharyngeal tissue is insufficient to create appropriately sized adhesion patches, J-planarians divide pre-pharyngeally (figures S5, S12). These pre-pharyngeal events account for the remaining 10% of J-planarian fissions in (10). Second, we observed that the area of the tail offspring from a J-planarian fragmentation can be used to predict the area of the corresponding trunk offspring due to a linear scaling, constraining where a possible second division plane can form. By comparing the observed and predicted trunk offspring area for a subset of the fragmentation events (figure S13), we verified that the linear scaling is a good predictor of the trunk offspring area given the tail offspring area. The pharynx was always found in the trunk offspring of imaged offspring from J-planarian fragmentations (n=21), demonstrating that a second division must be pre-pharyngeal (figure S12). Third, using the scaling of trunk area with tail area of fragmentations, we calculated the areas of a theoretical trunk (figure 7(a)) and head offspring (figure 7(b)) resulting from a theoretical second division in J-planarians that only fissioned, albeit being of comparable size to J-planarians that fragmented. We found that the areas of these theoretical head offspring were generally smaller than those of J-planarians that fragmented (figures 7(a-b)). This suggests that most of the planarians that only divided once did not have had sufficient pre-pharyngeal tissue for a second division. A small fraction of J-planarians appear to theoretically have had sufficient tissue to divide again and fragment, but did not do so, suggesting that other, non-mechanical factors influence the decision between fission versus fragmentation.

3.5.3.2. G-planarians

G-planarian fission is initiated by tail constriction, creating a popsicle-like shape. The area of the tail of the popsicle has a fixed proportionality to the parent area (figure 7(c)). We and others (9,24,25) have only observed post-pharyngeal divisions in this species, suggesting that, like J-planarians, G-planarians will not form a waist containing the pharynx. Considering G-planarian head offspring resulting from a fission, we find that there is insufficient post-pharyngeal tissue to form the constriction necessary for a second division (figures 7(d) and S5). Two of 22 (9%) G-planarians imaged post-division had sufficient post-pharyngeal tissue to potentially divide again (data points within the error bars in figure 7(d)), suggesting that this is the possible fragmentation

rate in this species. This is consistent with previous large scale population data showing that fragmentations account for 6% of G-planarian reproductive events (7).

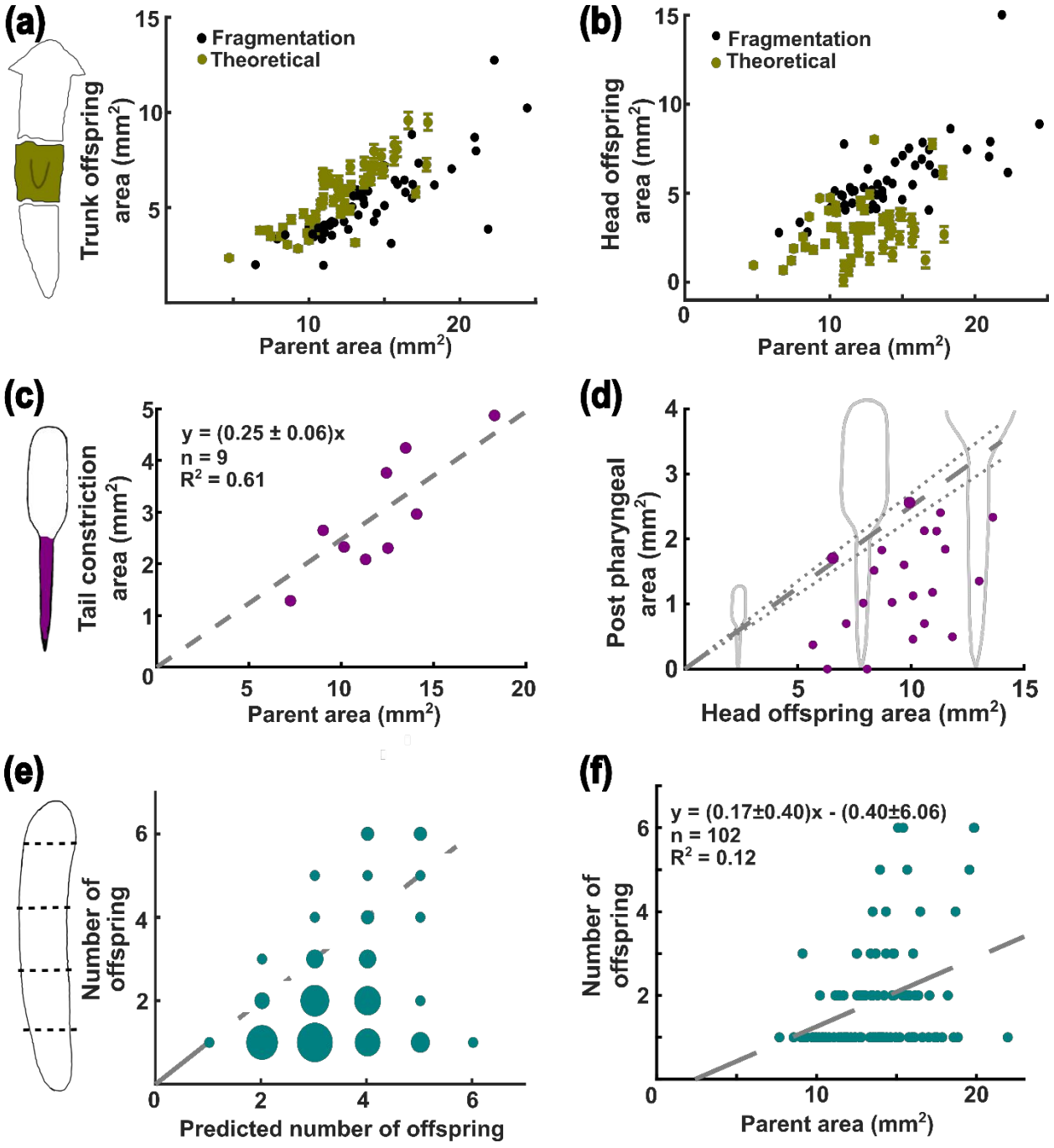

Figure 7. Offspring number is directed by constraints on waist formation. (a) Area of actual trunk offspring observed in fragmentation events and theoretical trunk offspring expected after fission events as a function of parent area for J-planarians. Error bars are twice the width of the standard error in

theoretical predictions. (b) Area of the actual head offspring observed in fragmentation events and theoretical head offspring expected in fission events as a function of the parent area. Most theoretical head offspring are smaller than those observed from fragmentation of J-planarians of comparable parent size. (c) Area of tail constriction as a function of gliding area of the parent G-planarian. Dashed line represents a linear fit, with the slope provided as mean ± standard deviation. (d) Area of the post-pharyngeal region of G-planarian head offspring immediately after division as a function of the head offspring area. The dashed line is $y = 0.25x$, corresponding to the linear fit line in (c). Dotted lines indicate the bounds of the standard error. Only planarians whose post-pharyngeal area lies above the lower dotted line would be able form a tail constriction of the required size to be able to fragment. Because the planarians were not observed post first division, we do not know whether the 2 worms that are big enough ultimately fragmented. (e) Experimentally observed number of offspring plotted against predicted number of offspring for n = 102 S-planarians. Offspring number is predicted by dividing the parent area by the average tail offspring area. Dashed line represents the 1:1 line for a visual guide. Size of circles corresponds to the frequency of a particular (x, y) pair. (f) Number of offspring as a function of parent area for S-planarians. Dashed line represents a linear fit, with the slope and intercept provided as mean ± standard deviation.

3.5.3.3. S-planarians

Unlike J- and G-planarians, S-planarians primarily fragment and produce multiple offspring per reproduction event. Since S-planarian tail/trunk offspring are of roughly constant size (figure 5(c) and figure S11), we can predict the number of offspring an S-planarian could theoretically produce by dividing the parent area by the average tail offspring area (figure 7(e)). Interestingly, this largely overpredicts the number of offspring produced (figures 7(e), S11(c)). S-planarian parent area and length only have a weak positive correlation with offspring number (figures 7(f), S11(d)), consistent with previous reports (4,6,11) and the number of offspring produced is highly variable for an S-planarian of a given size (figures 7(e), S11(c)). Thus, size is not a predictor of the number of offspring that will be produced, as even very large S-planarians sometimes only fission (figures 7(f), S11(d)) (4,6). These data suggest that - like what we observed for J-planarians - other, size-independent factors affect how many offspring are produced in a given reproductive event.

4. Discussion

Through continuous large-scale, long-term imaging at unprecedented temporal and spatial resolution, we investigated the mechanics of self-bisection across three planarian species (J-, G- and S-planarians). Two characteristics were found to be critical for division in all three species: 1) formation of a narrow waist to amplify stress and 2) the need for sufficient substrate adhesion to maintain the tensile stress in the waist to allow for rupture.

To our surprise, we found that the planarian species accomplished these tasks through distinct mechanisms. Most notably, how the waist forms differs across the species. J- and G-planarians

actively constrict their circular muscles at specific relative locations along the length of the worm (figure 2(a)). This constraint on where the waist forms directly dictates the distribution of biomass among the offspring, as evidenced by the scaling relationship of tail offspring to parent area (figure 5). In contrast, waist formation in S-planarians occurs primarily because of elongation and depends on the adhesion patches. S-planarians that lose adhesion and slip must restart the division process, whereas J- and G-planarians create and maintain their waist independently of the adhesion patches (figure S9).

While J- and G-planarians do not require the adhesion patches for waist formation, substrate adhesion is critical in all three species for successful rupture. All three species regulate their substrate adhesion in response to external forces to maintain offspring size (figure 6). These species have wide ecological ranges where they would encounter substrates of different physical properties (roughness, stiffness). However, changing substrates (soft and sticky PDMS versus hard and roughened plastic) had no obvious effects on fission dynamics, in agreement with the findings reported in (10), where J-planarian fission was studied on hard plastic and extremely soft PDMS, without any difference in dynamics. Since the size of the offspring influences their survival and reproductive success, it makes sense that the planarians can modulate other factors to maintain offspring size. Planarians interact with the substrate through a layer of secreted mucus. Thus, substrate adhesion can be regulated by changes to the quantity and/or composition of the mucus – something planarians also do in response to chemical exposure (10,21,26). Thus, we tried to modulate mucus by exposing the planarians to the detergent Triton-X 100, which was previously shown to increase mucus production and stickiness in J-planarians (10). However, because we can neither predict nor induce planarian self-bisection, this required long-term Triton-X 100 exposure which caused adverse health effects such that the planarians no longer divided.

Understanding how each of these planarian species self-bisects and the subsequent relationships between offspring and parent size allows us to predict the size of the posterior offspring for each species. For J- and G-planarians, if given the size of the parent, the tail offspring size can be predicted based on the demonstrated scaling relationship. The scaling relationship for J-planarians is only based on post-pharyngeal divisions, which constitute most division events. Pre-pharyngeal divisions are a small minority of division events (approximately 10%) and only occur in planarians with short RWTs which had insufficient time to reposition their pharynx (10). As previously shown (10), if given the relative pharynx location of the parent planarian, one can predict whether division will occur pre- or post-pharynx. This predictability allows for the development of theoretical growth models to explain the observed reproductive behavior (8).

S-planarian offspring size is roughly constant and thus also predictable. The observation that S-planarians generate multiple successive offspring of roughly constant size agrees with the recently proposed compression plane model (11)**.** The model proposes that S-planarians have

mechanically weak compression planes at regularly spaced intervals along the A-P axis that are used for rupture. While this idea cannot be tested directly because visualizing the compression planes kills the animal (11), we have observed that S-planarians often initially form multiple, evenly spaced temporary waists (figure S9(d)) until one is eventually "chosen" and used for rupture. These temporary waists could be indicative of the mechanically weak compression planes. It remains unclear what determines at which plane division will occur, as it is not always the most posterior waist that is "chosen". This stochastic element may contribute to the large variability observed in S-planarian offspring size.

In fact, across multiple parameters (RWT, number and size of offspring, timescales of fracture and recoil), S-planarians have noticeably greater variance than the other two species. We speculate that these differences are a direct consequence of the different division biomechanics: J- and G-planarians form their waist through active muscle contractions at specific locations whereas S-planarians first stretch, forming the waist at a structural weak point, which can only be maintained with the presence of adhesion patches. Thus, S-planarian self-bisection appears to be less controlled, leading to greater sources of variability.

We have demonstrated here that mechanical constraints can explain the observed reproductive behavior and lack of fragmentations in J- and G-planarians. However, worm area and/or mechanical constraints alone are not predictive of offspring number for S-planarians. Furthermore, the prediction for J-planarian behavior is not absolute; about 6% (n = 52) of imaged J-planarians would have been able to fragment based on the mechanical constraints but did not do so. This implies that other, non-mechanical mechanisms influence whether an individual planarian of sufficient size for fragmentation ultimately undergoes fission or fragmentation.

Biochemical signaling gradients may be the missing link to understand the stochasticity in the control of offspring number per reproductive event. A recent theoretical model has attempted to use biochemical gradients to explain where and when planarians divide based on a controlled, cross-inhibited Turing system (27). The model qualitatively explains several experimental observations: presence of fission and fragmentation, increase in fission activity upon decapitation and the relative size of the offspring (27). However, as a deterministic model, it cannot recapitulate the observed stochasticity in planarian division. Moreover, it is based on data and assumptions from multiple planarian species, which, as we have shown here, do not have the same reproductive behavior. These differences have clear effects on division location and thus need to be accounted for.

Several different signaling pathways may play roles in governing planarian asexual reproduction. Consistent with the Turing model, A-P axis polarity in S-planarians is maintained through self-organized Wnt gradients autonomously formed in the tail (28). A head-based patterning system that mutually inhibits the Wnt patterning system in the tail is also needed (28). Wnt and TGFβ

signaling have been implicated in controlling the frequency of division in S-planarians while Hox signaling has been shown to affect the number of compression planes and the spacing between them (11,12).

Most of this biochemical understanding has arisen from studies on S-planarians. While Wnt signaling has also been shown to be important for axial patterning in J- and G-planarians (29–31), it is unclear whether there are differences in gradient intensity or slope that may lead to the species-specific mechanisms that we have observed. In addition to morphogen gradients, positional control genes expressed in muscle cells have been shown to provide important positional cues, allowing the muscles to act as a coordinate system for tissue regeneration (32). Given the active role of muscle contraction in waist formation in J- and G-planarians, it is possible that muscle cells may set their own positional cues and then act upon them. In addition, the secreted trophic factor TCEN49 has been found to be necessary but not sufficient to induce fission in G-planarians, suggesting a potential role of the nervous system in fission induction (33). This neuronal control is likely regional as the brain is not required for division.

Together, these observations suggest that morphogen gradients, neuronal signals, and the biomechanical constraints shown here, cooperate to regulate when and where a planarian will divide. While the details of this cooperation will likely differ given the differences in reproductive strategies, key components of the process – such as the mechanical ones identified here (waist formation, substrate adhesion and tensile stress generation) – are expected to be universal. Two key experimental challenges must be overcome to further dissect this coordinated interplay between mechanical and biochemical signaling *in vivo*: 1) the ability to trigger fission on demand to record division with higher spatial and temporal resolution, and 2) *in vivo* labeling of proteins implicated in fission regulation.

Author Contributions

T.G. and D.I. performed data analysis and co-wrote the initial draft. V.S. performed data analysis. C.R. performed experiments. P.H.D co-designed the research. E.-M. S. C. designed and directed the research, performed experiments, and co-wrote the initial draft. All authors edited and co-wrote the final version of the manuscript.

Acknowledgments

The authors thank Ellen Adams for the planarian schematic, Kevin Bayingana for help with image analysis, Jared Talbot, Paul Malinowski and Darvin Ye for fission recordings, and Dr. Rui Wang and Ziad Sabry for help with monitoring fission recordings.

Funding

This work was funded by NSF CAREER Grant 1555109 (to EMSC), US DOE under Award No. DE − FG02 −04ER54738 (to P.H.D) and Swarthmore College. The funders had no role in the

design and conduct of the study, in the collection, analysis, and interpretation of the data, and in the preparation, review, or approval of the manuscript.

References

1. Rink JC, editor. Planarian regeneration: methods and protocols. New York, NY: Humana Press; 2018. 573 p. (Methods in molecular biology).

2. Cebrià F. Planarian Body-Wall Muscle: Regeneration and Function beyond a Simple Skeletal Support. Front Cell Dev Biol. 2016;4:8.

3. Hirshfeld A. The electric life of Michael Faraday. New York: Walker; 2006. 258 p.

4. Quinodoz S, Thomas MA, Dunkel J, Schötz E-M. The More the Merrier?: Entropy and Statistics of Asexual Reproduction in Freshwater Planarians. J Stat Phys. 2011 Apr;142(6):1324–36.

5. Dunkel J, Talbot J, Schötz E-M. Memory and obesity affect the population dynamics of asexual freshwater planarians. Phys Biol. 2011 Apr;8(2):026003.

6. Thomas MA, Quinodoz S, Schötz E-M. Size Matters!: Birth Size and a Size-Independent Stochastic Term Determine Asexual Reproduction Dynamics in Freshwater Planarians. J Stat Phys. 2012 Sep;148(4):664–76.

7. Carter JA, Lind CH, Truong MP, Collins E-MS. To Each His Own. J Stat Phys. 2015 Oct 1;161(1):250–72.

8. Yang X, Kaj KJ, Schwab DJ, Collins E-MS. Coordination of size-control, reproduction and generational memory in freshwater planarians. Phys Biol. 2017 May 23;14(3):036003.

9. Davison J. Population Growth in Planaria Dugesia tigrina (Gerard) : Regulation by the absolute number in the population. J Gen Physiol. 1973 Jun 1;61(6):767–85.

10. Malinowski PT, Cochet-Escartin O, Kaj KJ, Ronan E, Groisman A, Diamond PH, et al. Mechanics dictate where and how freshwater planarians fission. Proc Natl Acad Sci. 2017 Oct 10;114(41):10888–93.

11. Arnold CP, Benham-Pyle BW, Lange JJ, Wood CJ, Sánchez Alvarado A. Wnt and TGFβ coordinate growth and patterning to regulate size-dependent behaviour. Nature. 2019 Aug;572(7771):655–9.

12. Arnold CP, Lozano AM, Mann FG, Lange JJ, Seidel C, Alvarado AS. Hox genes regulate asexual reproductive behavior and tissue segmentation in adult animals. bioRxiv. 2021 Jan 1;2021.01.24.427972.

13. Cebrià F, Newmark PA. Planarian homologs of netrin and netrin receptor are required for proper regeneration of the central nervous system and the maintenance of nervous system architecture. Development. 2005 Aug 15;132(16):3691–703.

14. Morita M, Best JB. Effects of photoperiods and melatonin on planarian asexual reproduction. J Exp Zool. 1984;231(2):273–82.

15. Best JB, Goodman AB, Pigon A. Fissioning in Planarians: Control by the Brain. Science. 1969 May 2;164(3879):565–6.

16. Pigon A, Morita M, Best JB. Cephalic mechanism for social control of fissioning in planarians. II. Localization and identification of the receptors by electron micrographic and ablation studies. J Neurobiol. 1974;5(5):443–62.

17. Best JB, Abelein M, Kreutzer E, Pigon A. Cephalic mechanism for social control of fissioning in planarians: III. Central nervous system centers of facilitation and inhibition. J Comp Physiol Psychol. 1975;89(8):923–32.

18. Best JB, Morita M. Planarians as a model system for in vitro teratogenesis studies. Teratog Carcinog Mutagen. 1982;2(3–4):277–91.

19. Stowell NC, Goel T, Shetty V, Noveral J, Collins E-MS. Quantifying Planarian Behavior as an Introduction to Object Tracking and Signal Processing. The Biophysicist [Internet]. 2021 Apr 27 [cited 2021 Sep 14]; Available from: https://meridian.allenpress.com/the-biophysicist/article/doi/10.35459/tbp.2020.000159/464616/Quantifying-Planarian-Behavior-as-an-Introduction

20. Schindelin J, Arganda-Carreras I, Frise E, Kaynig V, Longair M, Pietzsch T, et al. Fiji: an open-source platform for biological-image analysis. Nat Methods. 2012 Jul;9(7):676–82.

21. Ireland D, Bochenek V, Chaiken D, Rabeler C, Onoe S, Soni A, et al. Dugesia japonica is the best suited of three planarian species for high-throughput toxicology screening. Chemosphere. 2020 Aug 1;253:126718.

22. Cochet-Escartin O, Mickolajczyk KJ, Collins E-MS. Scrunching: a novel escape gait in planarians. Phys Biol. 2015 Sep 10;12(5):056010.

23. Sikes JM, Bely AE. Radical modification of the A-P axis and the evolution of asexual reproduction in Convolutriloba acoels. Evol Dev. 2008 Oct;10(5):619–31.

24. Mead RW. Proportioning and regeneration in fissioned and unfissioned individuals of the planarian Dugesia tigrina. J Exp Zool. 1985;235(1):45–54.

25. Sheĭman IM, Sedel'nikov ZV, Shkutin MF, Kreshchenko ND. [Asexual reproduction of planarians: metric studies]. Ontogenez. 2006 Apr;37(2):130–5.

26. Hagstrom D, Zhang S, Ho A, Tsai ES, Radić Z, Jahromi A, et al. Planarian cholinesterase: molecular and functional characterization of an evolutionarily ancient enzyme to study organophosphorus pesticide toxicity. Arch Toxicol. 2018 Mar 1;92(3):1161–76.

27. Herath S, Lobo D. Cross-inhibition of Turing patterns explains the self-organized regulatory mechanism of planarian fission. J Theor Biol. 2020 Jan;485:110042–110042.

28. Stückemann T, Cleland JP, Werner S, Thi-Kim Vu H, Bayersdorf R, Liu S-Y, et al. Antagonistic Self-Organizing Patterning Systems Control Maintenance and Regeneration of the Anteroposterior Axis in Planarians. Dev Cell. 2017 Feb 6;40(3):248-263.e4.

29. Marsal M, Pineda D, Saló E. Gtwnt-5 a member of the wnt family expressed in a subpopulation of the nervous system of the planarian Girardia tigrina. Gene Expr Patterns GEP. 2003 Aug;3(4):489–95.

30. Yazawa S, Umesono Y, Hayashi T, Tarui H, Agata K. Planarian Hedgehog/Patched establishes anterior-posterior polarity by regulating Wnt signaling. Proc Natl Acad Sci U S A. 2009 Dec 29;106(52):22329–34.

31. Umesono Y, Tasaki J, Nishimura Y, Hrouda M, Kawaguchi E, Yazawa S, et al. The molecular logic for planarian regeneration along the anterior–posterior axis. Nature. 2013 Aug;500(7460):73–6.

32. Witchley JN, Mayer M, Wagner DE, Owen JH, Reddien PW. Muscle Cells Provide Instructions for Planarian Regeneration. Cell Rep. 2013 Aug 29;4(4):633–41.

33. Bueno D, Fernàndez-Rodríguez J, Cardona A, Hernàndez-Hernàndez V, Romero R. A novel invertebrate trophic factor related to invertebrate neurotrophins is involved in planarian body regional survival and asexual reproduction. Dev Biol. 2002 Dec 15;252(2):188–201.